September 2025
Volume 1
Issue 3

DOI: 10.48308/ijce.2026.243172.1018

# Machine Learning-Aided Rapid Seismic Damage Level Identification for Reinforced Concrete Columns Using Succolarity and Lacunarity

**Authors:**

**Mohammad Javad Hamidia*[1], Samira Azhari[1]**

## Abstract

The traditional method for seismic damage assessment is visual inspection, which is risky and prone to human mistakes. A quick and non-contact approach for predicting the seismic damage status of buildings is crucial for automated inspection immediately after earthquakes. In this paper, damage level prediction using crack image analysis and machine learning is presented. Two aspects of texture complexity, including Succolarity and Lacunarity, are measured in order to quantify surface damage. FEMA P-58-compliant damage level and repair activity prediction models are generated by training a variety of algorithms utilizing a collected experimental database. The input features of the algorithms are selected as geometric characteristics, structural parameters, and image-extracted indices. Five-fold cross-validation is used to evaluate models for overfitting and generalizability. Among the considered algorithms, CatBoost outperforms for the case where the inputs are Succularity, Lacunarity, and the aspect ratio. Five-fold cross-validation results show that the classification model are not overfit.

**Keywords:** Succolarity, Lacunarity, Seismic Damage, RC Column, Machine Learning

1. Faculty of Civil, Water, and Environmental Engineering, Shahid Beheshti University, Tehran, Iran

*Corresponding Author: m_hamidia@sbu.ac.ir

## 1. Introduction

By using real-time damage analysis, the post-earthquake loss analysis eliminates uncertainty. Following an earthquake, the typical approach for determining the extent of damage and assessing the safety of buildings has been a visual assessment by an expert, carried out in accordance with established guidelines (Rojah 2005). Following an earthquake, aftershocks can cause serious damage to buildings. Buildings that were previously damaged during the main shock are more vulnerable. According to the rule about "entering damaged buildings," buildings with "red" and "yellow" tags cannot be entered (Reasenberg, Poland, and Engineers). The destructive aftershocks of the previous earthquake caused some buildings to collapse (Asayesh et al. 2023; Babaie Mahani and Kazemian 2018; Barbot et al. 2023).

Such a subjective manual process is dangerous for seriously damaged structures and is prone to human mistakes. By offering a quick, integrated, non-contact evaluation of structural safety and a way to identify repairs following an earthquake, automated techniques get around the drawbacks of visual inspection. In order to determine the best post-earthquake repair technique to reduce recovery times, it is also crucial to quickly and accurately analyze the seismic damage to buildings.

Determining the degree of damage to reinforced concrete (RC) columns is crucial for assessing the stability and serviceability of structures, as well as for choosing the method of repairs (FEMA 306, 1998) after an earthquake. For the RC components, FEMA P-58 (Birely, Lowes, and Lehman 2011) created category seismic damage states (DSs) based on the degree of damage and suggested method of repairs (MoRs). The growth of cracks and concrete crushing are the most obvious signs of damage to RC components. This paper builds damage quantification utilizing damage pattern characteristics and applies it to a machine learning framework for post-earthquake DS and MoR prediction of damaged RC columns.

## 2. Literature Review

Following the damage recognition of the damage pattern using the automated methods (Alamdari and Ebrahimkhanlou 2024; Cordeiro and Leonel 2019; Hu et al. 2021; Y. Liu and Yeoh 2021; Nanthakumar et al. 2016; Shamsabadi et al. 2022; Xiang et al. 2022; Zhou, Rabczuk, and Zhuang 2018; Z. Zhu, German, and Brilakis 2011), the damage indices are needed to classify the damage. Many researchers used image processing techniques to address the measurement of crack and crushing severity in the quantification phase. The degree of damage to the structural elements is influenced by the complexity of the damage, in addition to its quantity. Several image-based indices have been established in order to measure the properties of the texture patterns in the images. Fractal dimensions can be used to measure distribution probability and pattern complexity (Mandelbrot 1967) based on the Rényi entropy (Rényi 1961). In order to measure damage in RC components, fractal dimensions of surface

crack maps have also been widely used (Athanasiou et al. 2020; D. Zhu et al. 2021). For example, the peak drift ratio in RC columns has been predicted using fractal dimensions (Jamshidian and Hamidia 2023).

Succolarity and Lacunarity are designed as image-based indices to extract more important characteristics of the textures [50]. The Succolarity and Lacunarity quantify the texture's connection and the pattern's distribution throughout the image, respectively (Rafael H C de Melo and Conci 2013; Plotnick, Gardner, and O'Neill 1993). These indices have been used for image texture analysis in many different study domains (Grzybowski and BLACHOWICZ 2020; Hassan et al. 2015; Rafael Heitor Correia de Melo 2007; Xia et al. 2019; Zhao et al. 2021).

Recently, techniques based on data to predict the seismic response in structures/components have made substantial use of machine learning (ML) algorithms. Without requiring extensive numerical and experimental research, the ML-based data-driven methods will be trained using the data to generate the damage classification models for structural components (Huang and Burton 2019; Mangalathu and Jeon 2018; Nguyen et al. 2021; Olalusi and Spyridis 2020; Rajakarunakaran et al. 2022; Zhang et al. 2020). For damage assessment after the earthquakes, the most useful inputs for ML algorithms are the image-based features (Lattanzi et al. 2016; Paal et al. 2015).

Surface crack maps of RC components were also used to categorize the failure mode and DS (Azhari et al. 2025; Azhari and Hamidia 2024). Chen et al. proposed ML learning-based DS prediction for structural walls using the structural parameters, crack, and image-based features (Q. Chen, Yu, and Li 2024). Neural networks have been employed for the detection of damage on RC components (Harirchian, Lahmer, and Rasulzade 2020; Moradi and Hariri-Ardebili 2019; Oh et al. 2020; Vafaei, Adnan, and Abd. Rahman 2013). The main purpose of this paper is to automate post-earthquake inspection in order to determine the DS for RC columns after an earthquake using characteristics of surface crack patterns.

## 3. Database

In this paper, a database of 448 RC columns is gathered from experimental tests in order to train the prediction model. The data points include 111 RC columns with rectangular cross-sections with double-curvature deformation shapes that were evaluated at various damage levels after being subjected to quasi-static cycle loads. The database contains geometric features, crack patterns, and structural properties of RC columns. Both axial and lateral loadings were applied to the specimens.

Figure 1 displays the relative frequencies of the database attributes. Specimens exhibiting a variety of structural design characteristics are included in the database. Throughout the tests,

drift ratios of up to 6.00% were recorded in the RC columns. The geometric and structural characteristics of the databank are listed in Table 1.

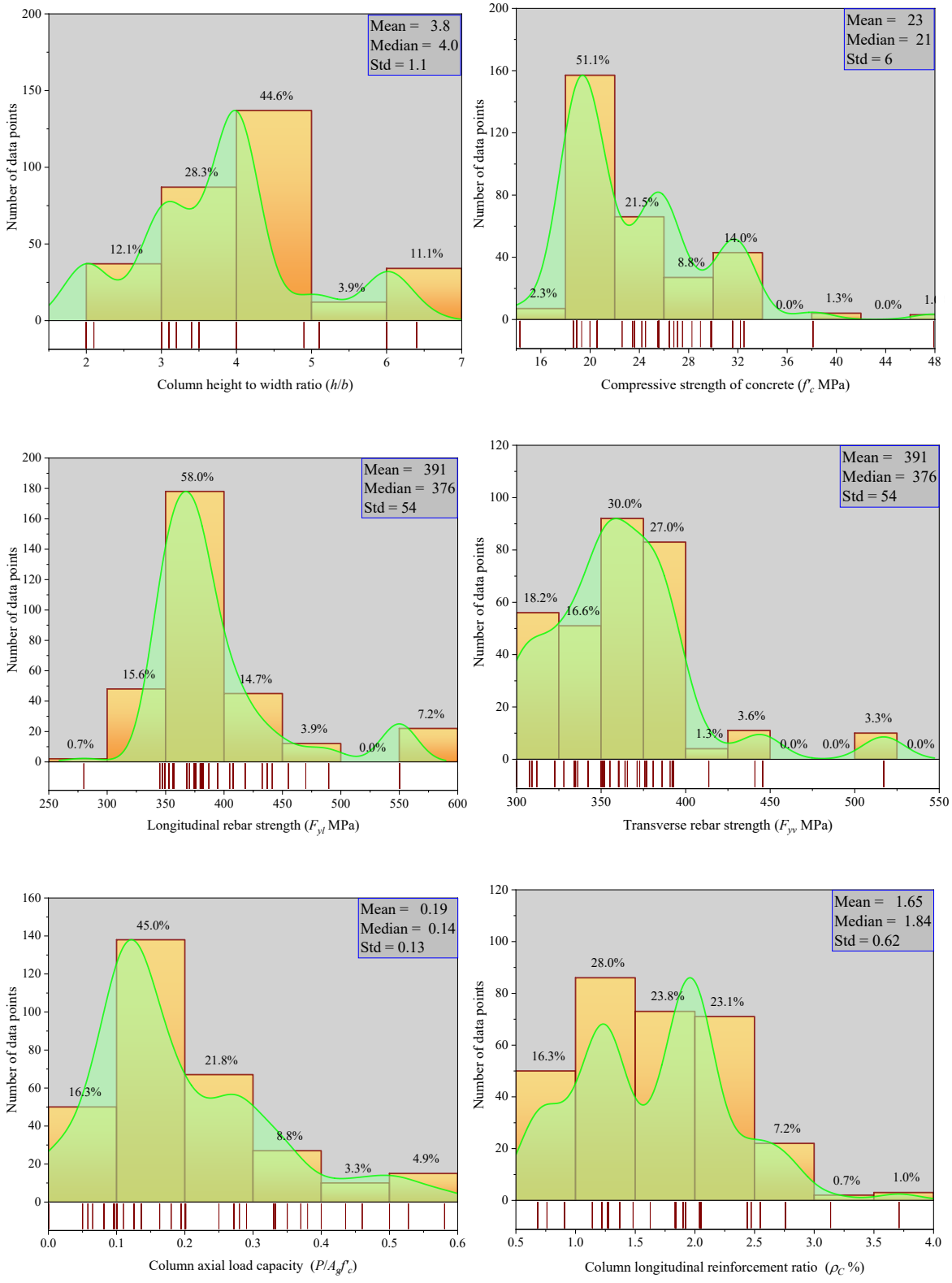

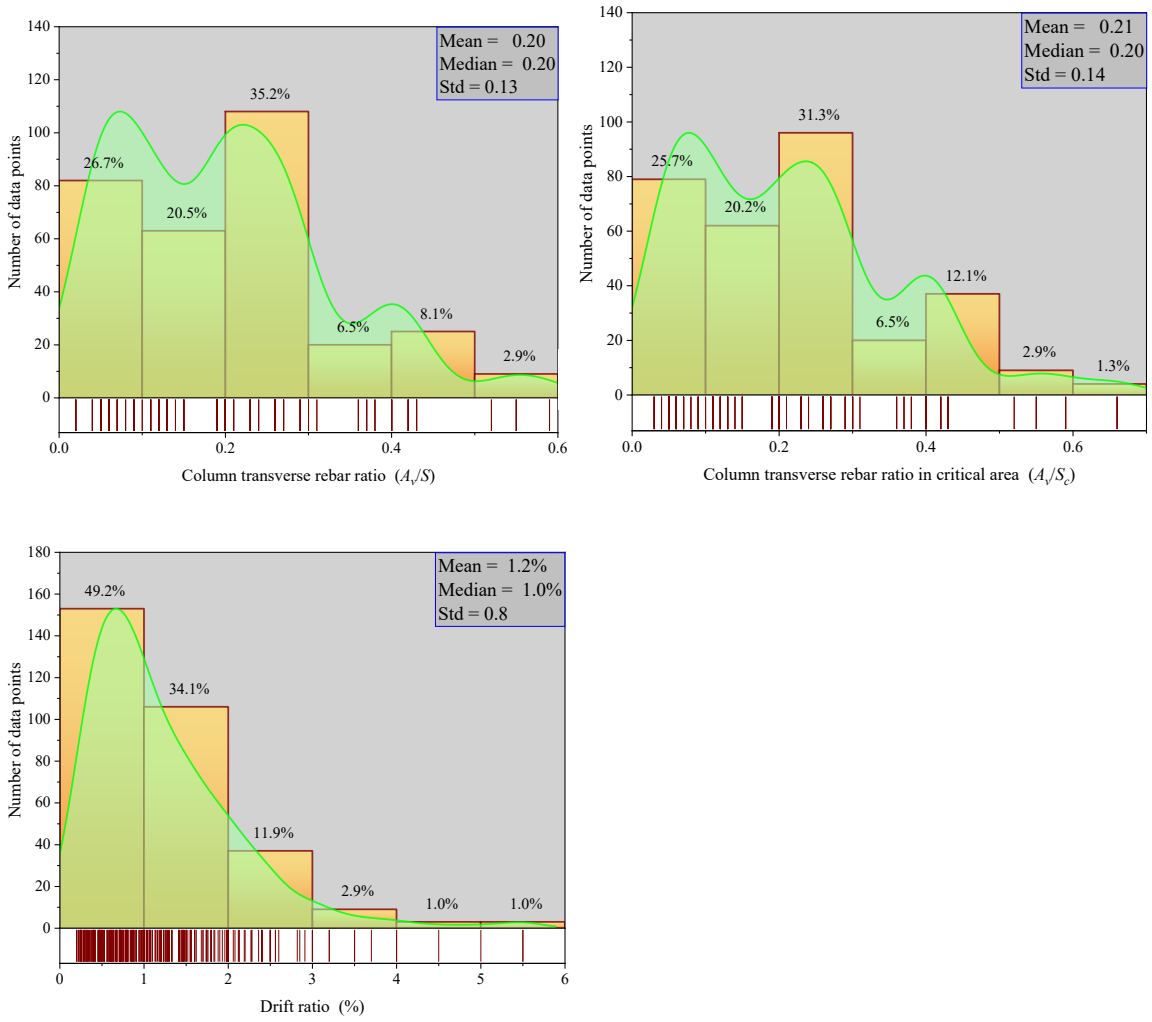


**Figures 1. Database characteristics and distributions**

**Table 1. Summary of the database**

| Reference | $\frac{P}{A_g f_c'}$ | $f_c'$ (MPa) | $\rho_C$ (%) | *Fyl* (MPa) | *Fyv* (MPa) | $\frac{A_v^*}{S}$ (cm) | *h/b* | No. of data points |
|---|---|---|---|---|---|---|---|---|
| (Lynn et al. 1996) | 0.28 | 26 | 3.1 | 280 | 517 | 0.06 | 6.4 | 2 |
| (Bett, Jirsa, and Klingner 1985) | 0.53 | 30 | 0.8 | 490 | 414 | 0.13 | 2.1 | 4 |
| (Lim et al. 2016) | 0.06-0.10 | 48-58 | 3.5-3.7 | 470 | 441-486 | 0.38-0.52 | 3.0-4.0 | 6 |
| (Son 2018) | 0.06-0.40 | 32-38 | 2.1 | 550 | 300 | 0.20-0.40 | 3.1-5.1 | 38 |
| (Henkhaus 2010) | 0.11-0.46 | 19-29 | 1.5-2.5 | 441-490 | 517 | 0.02-0.05 | 3.2-6.4 | 13 |
| (Tran 2010) | 0.05-0.50 | 23-33 | 2.1 | 408 | 393 | 0.05 | 3.4-4.9 | 39 |
| (Yamamoto and Munemura 1974) | 0.00-0.33 | 19 | 1.2-2.8 | 347-370 | 309-392 | 0.05-0.59 | 2.0-4.0 | 67 |
| (Omor et al. 1974) | 0.08-0.19 | 27-32 | 0.9-2.6 | 344-381 | 334-386 | 0.06-0.37 | 2.0-4.0 | 46 |
| (Osamu et al. 1974) | 0.14-0.27 | 19 | 0. 7-1.9 | 349-374 | 312-381 | 0.40-0.55 | 3.0-6.0 | 70 |
| (Azuma and Zenriku 1977) | 0.13-0.58 | 14-24 | 0.7-1.9 | 380-437 | 328-446 | 0.07-0.42 | 2.0-4.0 | 46 |
| (Fukada 1976) | 0.10-0.20 | 21-26 | 1.1-2.4 | 349-395 | 308-364 | 0.11-0.43 | 3.0-4.0 | 117 |

FEMA P-58 has summarized seismic damage of RC columns in six groups. Visual properties of damage and structural response are the basis of the damage classification criteria listed in FEMA P-58. DSs are reclassified into four classes in this paper, each of which corresponds to a MoR, and the specimens of the database are labeled based on these attributes. The DSs and MoRs as defined by FEMA P-58 are shown in Figure 2. The specimen AF-42TA (Yamamoto and Munemura 1974) at four drift ratios is also depicted in this picture.

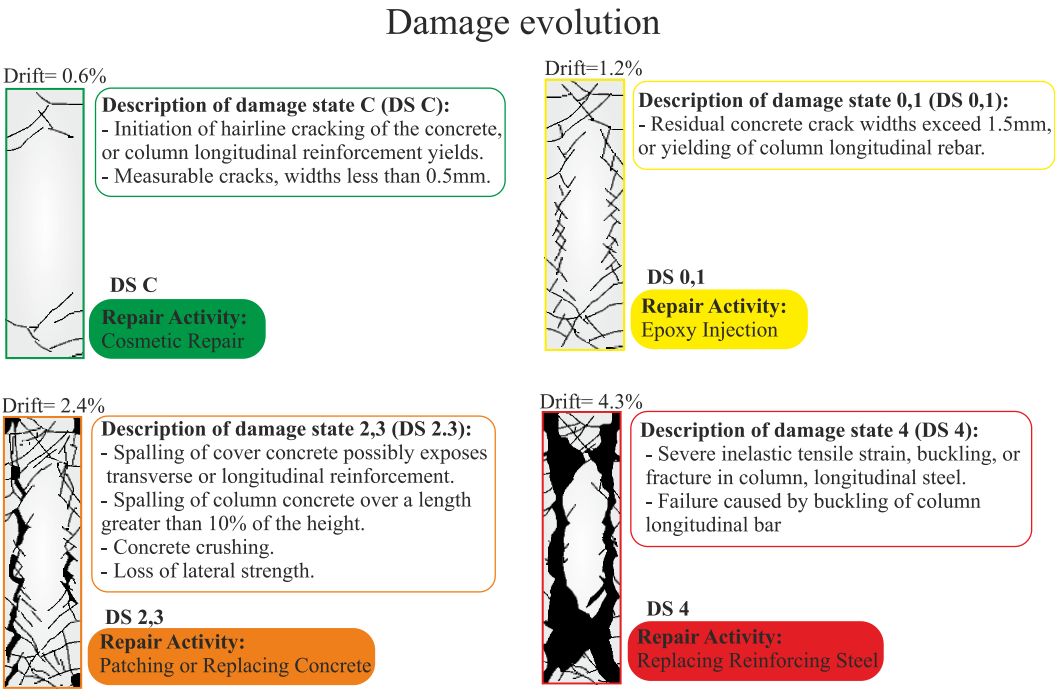


**Figure 2. DS description and corresponding MoRs**

Figure 3(a) shows the relative frequency histogram for the databank in each of the aforementioned DSs. Figure 3(b) displays the variation in the drift ratio for each DS. There is a noticeable trend in the drift ratio at the beginning and end of each DS. From DSC to DS4, the median drift ratio increases, as indicated by the filled marks in Figure 3(b). According to the experimental data, the four DSs have median drift ratios of 0.42%, 1.27%, 2.64%, and 3.50%, respectively.

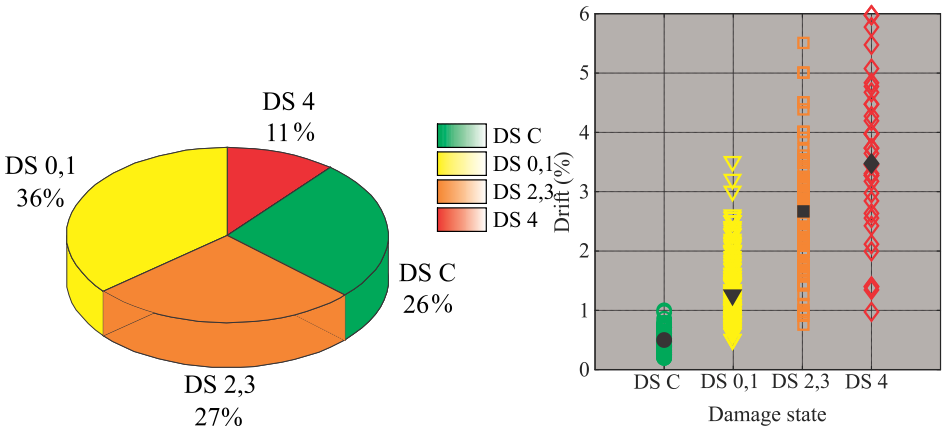


**Figure 3. Frequency of the DSs in the database and distribution of each DS versus the drift ratio**

## 4. Image-Based Indices

The indices are required to quantify the density and distribution of the damage throughout the photographs in order to capture the damage evolution and quantification following seismic

loading. A specimen with varying degrees of damage is depicted in Figure 4. As can be seen, cracks first appear at the specimen's top and bottom before spreading to its sides. Therefore, the indices utilized should be sensitive to the texture's direction and distribution for accurate quantification. Succolarity and Lacunarity are two texture complexity criteria that have been employed in this paper to quantify the complexity and irregularity of texture patterns. Succolarity and Lacunarity can be used jointly to quantify differences in the patterns' connections between two images with identical texture densities. In order to accurately identify the crack length and spatial distribution of the RC column surface crack textures and patterns, this paper explores the use of Lacunarity and Succolarity.

Lacunarity can be used to calculate the uniformity of pattern distribution across the image. This index takes into account the texture's density and variance for a particular pattern. Because Sucolarity is calculated in several directions, it is sensitive to the direction of texture qualities, whereas Lacunarity is not. Therefore, it is possible to determine the zones where the damages are concentrated. The techniques used to compute the previously mentioned texture complexity features are described in the following sections.

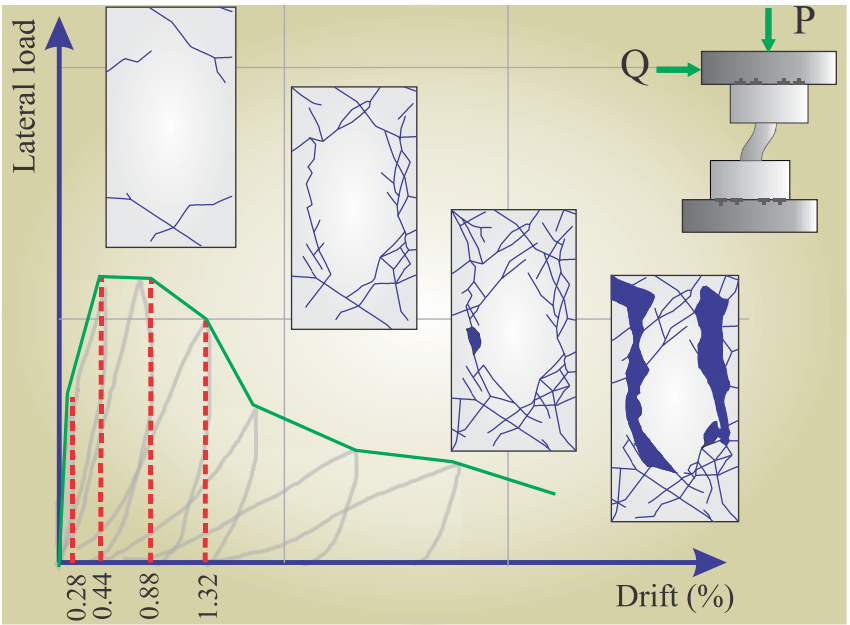


**Figure 4. Damage evolution in a specimen**

### 4.1. Succolarity Measurement

The fundamental idea for calculating Succolarity is the imaginary fluid flowing across the desired texture (Rafael Heitor Correia de Melo 2007). Damaged areas in RC columns are assumed to be fluid-penetrable, and it should be evaluated the capacity and pressure of flow across the texture. The digitalized images are converted into a binary matrix, where the number "1" represents the damaged pixels. The image's undamaged portions remain impervious. "0" in the binary matrix represents the image's pixels that are not part of the pattern. To determine the fluid pressure and capacity, the matrix is divided into boxes of identical size (BS). The box-

counting technique counts the pixels in each fluid-containing box (Russell, Hanson, and Ott 1980). The occupation percentage (*OP*) of a given box is determined by dividing the number of filled pixels by the total number of pixels.

Succolarity varies in different directions due to the flow pressure (*PR*), whereas the *OP* remains constant for all flow directions. *PR* increases linearly as the fluid advances. The flow pressure is measured at the boxes' middle point. For every box ($i$=1,...,$n$), *PR* and *OP* are found, and the Succolarity can be calculated using Equation (1) for the given direction, *dir*. In Equation (1), $\sum_{i=1}^{n}(OPi \times PRi)_{\max}$ is calculated under the assumption that all pixels contain fluid.

$$\text{.Succolarity} = \frac{\sum_{i=1}^{n} OPi \times PRi}{\sum_{i=1}^{n}(OPi \times PRi)_{\max}} \tag{1}$$

The top and bottom sections of RC columns have nearly identical damage patterns, according to the observation. It is important to note that the specimen's half-height picture is sufficient to determine the texture complexity features. The fluid direction for Succolarity in this research is considered to be bottom-to-above for the top section and above-to-bottom for the bottom section, as shown in Figure 5 for the specimen WS2-7B-H (Omor et al. 1974). The specimen's Succolarity is determined by averaging the TB and BT values for each column.

Figure 5(b) displays the *OP* for an example damage pattern of the upper portion of Figure 5(a), taking into account 32 boxes on the image, each containing 128x128 pixels. Additionally, the *PR* in the center of the boxes in the bottom-to-above direction is shown by the crack pattern in Figure 5(a). As seen in Figure 5(a), the pressure is the same for the boxes in the same row.

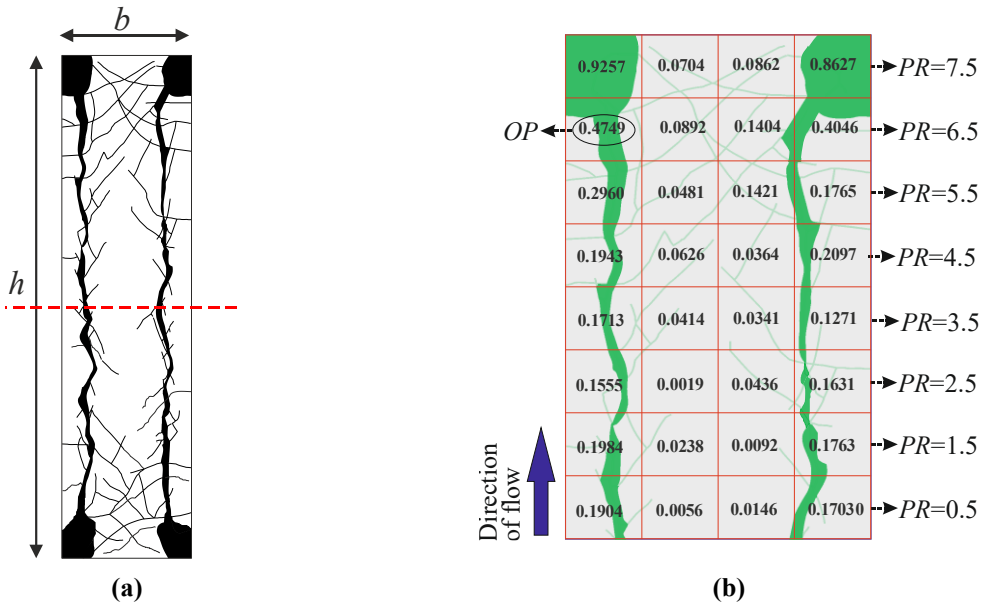

**Figure 5. Crack map and Succolarity calculation for the top section of a specimen from the database**

## 4.2. Lacunarity Measurement

The gliding box methodology is employed in this study to calculate Lacunarity; the box-counting method is applied each time the reference box glides (Allain and Cloitre 1991). To demonstrate the computing idea, Figure 6 shows an example of a matrix that was extracted from a specimen's binary matrix. The count of filled pixels inside the gliding box is counted, $m$. $N(m,r)$ is the number of pixels with a portion of damage inside the box (with the size of $r$). The gliding box must glide $N(r)$ times over the binary matrix, Equation (2). Equation (3) can be used to compute Lacunarity for a pattern.

$$N(r) = [\text{image width} - r + 1] \times [\text{image height} - r + 1] \quad \text{(all dimension in pixel)} \tag{2}$$

$$\text{Lacunarity} := \frac{\sum_m m^2 \frac{N(m,r)}{N(r)}}{\left[\sum_m m \frac{N(m,r)}{N(r)}\right]^2} \tag{3}$$

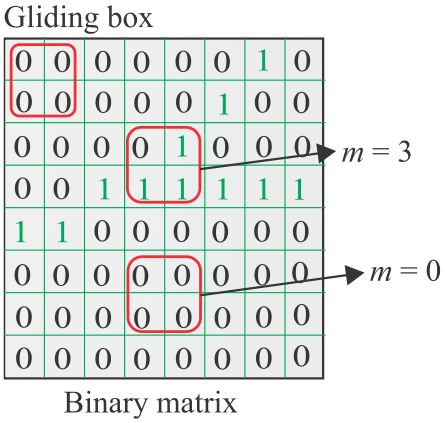


**Figure 6. Gliding-box example for Lacunarity calculation**

Figure 7 displays the variation of Lacunarity and Succolarity in relation to the drift for the specimen AF-42TA (Yamamoto and Munemura 1974). This figure indicates that the Succolarity trend increases as a result of the initial crushing. This tendency is brought on by an increase in the hypothetical flow's capacity. The Lacunarity plot exhibits a decreasing tendency before the crushing, as shown in Figure 7. Lacunarity increases with increased texture density once the concrete is crushed. The Lacunarity, which depends on density and heterogeneity, is influenced by the distribution of damage on the specimen. The gap size is influenced by both crushing and crack formation; however, there is less variability when the damage is localized in the specimen. The damage is localized when crushing begins, and how the crushing spreads across the column will influence how the Lacunarity trend shifts. To sum up, in order to offer more accurate damage quantification, the Lacunarity must be used with Succolarity.

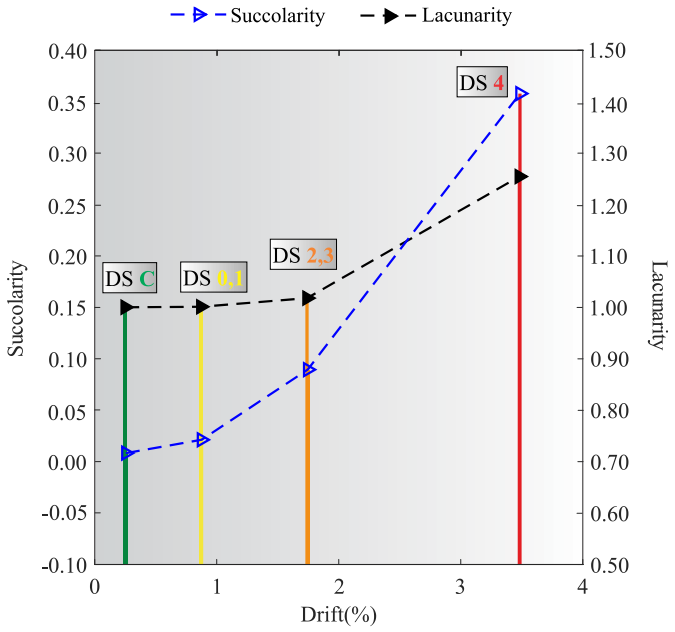


**Figure 7. Variation of Succolarity and Lacunarity for specimen AF-42TA (Yamamoto and Munemura 1974) with drift ratio**

The authors consider 20 pixels/centimeter as a scale factor. Figure 8 displays the ranges Succolarity and Lacunarity of images for all data points in each DS; the legend next to each plot indicates the quantity of the data points. The ranges of Lacuarity widen as one moves from DS C to DS 4; the initiation of DS C, DS 0,1, and DS 2,3 are distinguishable, and the median value of all DSs is higher than the minimum value of the earlier DSs. Succolarity and Lacunarity deviations are minimal for DS C. The plots in Figure 8 with red markers also show the ranges of the Lacunarity and Succolarity for the DSs where median values are found. The median Succolarity values in the RC column specimens increase with increasing damage levels. The observed trend demonstrates the true relationship between damage levels and the retrieved indices from the damage patterns. Also, Pearson and Spearman correlation coefficients of the drift ratio with Succolarity.

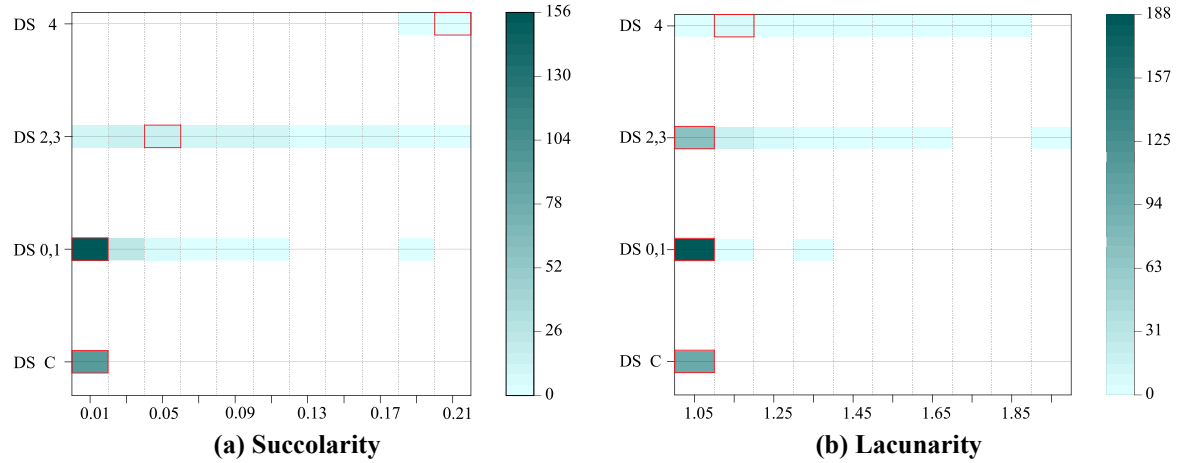


**Figure 8. Ranges for Succolarity and Lacunarity in DSs for all the databank images**

## 5. Supervised Learning Algorithms

The classification models in this study are trained using supervised learning. The five shallow learning algorithms are used. Single, boosting, and bagging learning processes are covered by the chosen algorithms. a) Random forest (RF) uses an ensemble technique to combine the output of multiple concurrent decision tree predictors. The class with the highest votes determines the categorization outcome through a bagging process (Breiman 2001; Géron 2022; Wager and Athey 2018). b) K-nearest neighbors (KNN) KNN algorithm represents each data point in an *n*-dimensional space from the training dataset with *n* characteristics. A new data point's anticipated class is the majority of the class of *N* data points that are closer to it (Chaudhuri and Dasgupta 2014; Cover and Hart 1967; Hart, Stork, and Duda 2000). c) boosting algorithms, including **CatBoost (CB), Extreme gradient boosting (XGB), Gradient boosting (GB):** Boosting is a method that employs successive models, each of which reduces the error associated with the data points that the preceding model incorrectly identified. To achieve the necessary degree of performance and complexity, the categorization is continuously improved by repeated learning (Alpaydin 2020; Friedman 2001; Hastie et al. 2009; Schapire and Freund 2013).

The training and testing datasets are chosen at random from the entire databank. The training dataset in this study consists of 70% of data points in each DS. Each algorithm is trained using the training dataset, using the image indices as predictors and DSs as output. The testing dataset's actual and predicted classes are compared to determine the accuracy of prediction. Additionally, the overfitting of the models is evaluated using five-fold cross-validation.

There are a number of customizable parameters for ML algorithms, and choosing different parameters have an impact on the model's performance. The optimal set of parameters must be selected during the training phase in order to determine the most accurate model. The ideal set of parameters (hyperparameters) is greatly influenced by the characteristics of the dataset. Based on a preset set of parameter values, an algorithm automatically selects two ideal parameters. The GridSearchCV looks through all possible combinations of the predefined variables based on the cross-validation score. The hyperparameters in this study are determined using scikit-learn's GridSearchCV tool. Three situations are used to feed the Succolarity and Lacunarity into the shallow learning-based classification models. In the first scenario, Succolarity is the input feature; in the second scenario, Lacunarity is selected as the input feature. In the last scenario, the inputs of the algorithms are both indices. In all scenarios, $h/b$ is also among the inputs.

The image-based characteristics are used as input for the five shallow learning algorithms that were previously introduced. To evaluate the performance of each algorithm in every situation, confusion matrices are used. The testing dataset confusion matrices and performance metrics for the algorithm with high accuracy in each of the scenarios taken into consideration are

displayed in Figure 9. The number of samples in each class that are really predicted is shown by the items on the principal diagonal of a confusion matrix. The quantity of data points whose classes are incorrectly predicted is displayed by other elements. The confusion matrices in Figure 9 display the metrics of "accuracy," "recall," and "precision."

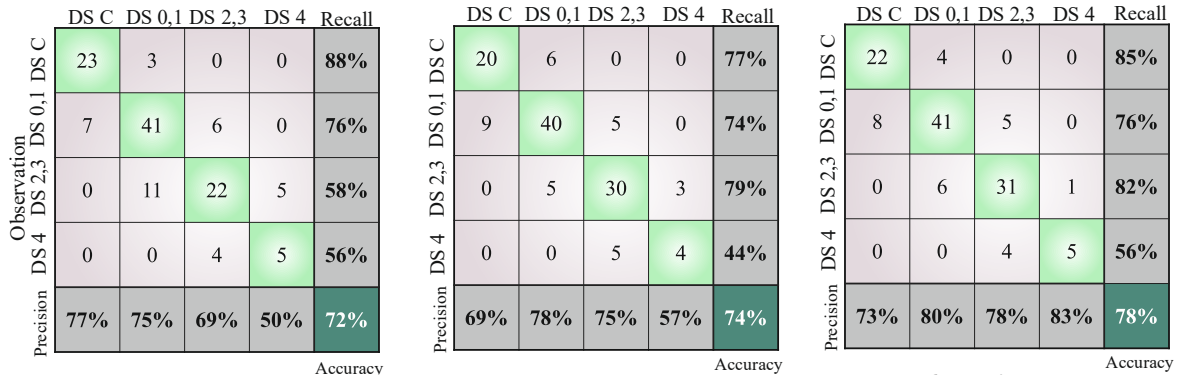


**(a) Scenario I-RF** **(b) Scenario II-GB** **(c) Scenario III-CB**

**Figure 9. Confusion matrices for the testing dataset**

For DS classification models, Scenario III in the CB algorithm has the highest accuracy (78%). It is necessary to prevent some misclassifications in the categorization difficulties. Predicting DS 4 as DS C, for example, may lead to mistakes in the loss estimation procedure and the incorrect repair action. Such mistakes are absent from the confusion matrices of scenarios I, II, and III. Fifteen confusion matrices that take into account five shallow-learning techniques for three scenarios are generated for the testing dataset.

Five-fold cross-validation is used in this study to evaluate the model's vulnerability to overfitting. An overfitted model matches the training data exactly but is overly complicated. The training dataset is divided into K folds at random in K-fold cross-validation. The model is trained using K-1 folds, and one of the folds is used for validation (Murphy 2022). The "accuracy" of K models is calculated after the process is repeated K times with different validation and training folds. The accuracy of the model for a particular training set can be determined by repeating this process. The significant differences between the five obtained accuracies point to an overfitting problem. The literature uses K-fold cross-validation to assess the likelihood of overfitting (Alpaydin 2020; Friedman 2001; Hastie et al. 2009; Schapire and Freund 2013). A five-fold cross-validation is performed for all cases, and the results are shown in Figure 10.

The changes in "accuracy" across different training folds are indicated by the height of the box chart. As the height of the boxes increases, ML models tend to overfit. Thus, scenarios III with algorithm CB perform the best.

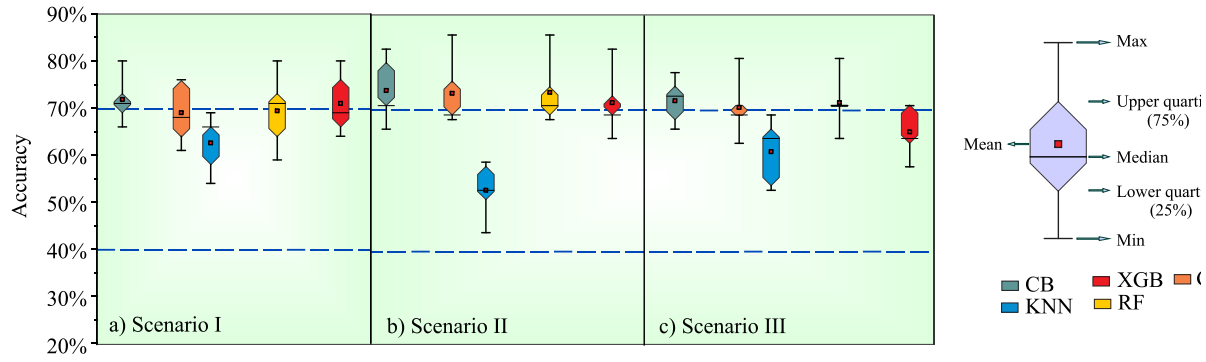


**Figure 10. K-fold cross-validation**

## 6. Summary and Conclusion

In this research, computer vision techniques are used to establish an automated safe damage state and repair method identification model for the RC columns. The primary application of this method is the quick decision-making for the repair technique of components using the image of the damaged components. The automated process shortens the typical recovery time for cities and structures, and the methodology allows for the adoption of more dependable restoration actions.

To train and evaluate classification models, a large number of photos showing the surface crack of damaged RC columns under cyclic stress are gathered from the literature. The authors classified the 448 images in the databank using the adopted repair actions and damage states defined in FEMA P-58. To measure the degree of damage to the specimens, two mathematical image intricacy indices are computed: Lacunarity and Succolarity of the crack maps. Five models based on supervised learning are used to train a damage-level classification model. Furthermore, three scenarios are presented for supervised learning feature selection. The GridsearchCV function adjusts the algorithm's parameters to maximize the models' performance.

- As the damage in a specimen progresses, Succolarity quantity increases.
- Among all models, the highest accuracy is obtained in scenario III with a value of 78% employing CB algorithm. In this scenario, the input features are Succolarity, Lacunarity, and the aspect ratio of columns.
- Generalizability evaluation of the selected model in scenario III with five-fold cross-validation achieves accuracy values ranging from 77% to 88% with a median of 78%, showing the overfitting prevention.

In conclusion, automated post-earthquake damage evaluation is the main use of damage state identification methodology. Decision-makers can choose and propose a repair plan by using the approach for the images of RC building components.

### Data Statement

Data will be made available on reasonable request.

### Conflict of Interest

The authors declare that there is no conflict of interest regarding the publication of this paper.

## 7. References

Alamdari, Ali Ghadimzadeh, and Arvin Ebrahimkhanlou. 2024. "A Multi-Scale Robotic Approach for Precise Crack Measurement in Concrete Structures." *Automation in Construction* 158: 105215.

Ali, Raza, Joon Huang Chuah, Mohamad Sofian Abu Talip, Norrima Mokhtar, and Muhammad Ali Shoaib. 2022. "Structural Crack Detection Using Deep Convolutional Neural Networks." *Automation in Construction* 133: 103989.

Allain, Cloitre, and M Cloitre. 1991. "Characterizing the Lacunarity of Random and Deterministic Fractal Sets." *Physical review A* 44(6): 3552.

Alpaydin, Ethem. 2020. *Introduction to Machine Learning*. MIT press.

Asayesh, Behnam M, Hamid Zafarani, Sebastian Hainzl, and Shubham Sharma. 2023. "Effects of Large Aftershocks on Spatial Aftershock Forecasts during the 2017–2019 Western Iran Sequence." *Geophysical Journal International* 232(1): 147–61.

Athanasiou, Apostolos, Arvin Ebrahimkhanlou, Jarrod Zaborac, Trevor Hrynyk, and Salvatore Salamone. 2020. "A Machine Learning Approach Based on Multifractal Features for Crack Assessment of Reinforced Concrete Shells." *Computer-Aided Civil and Infrastructure Engineering* 35(6): 565–78.

Azhari, Samira, and Mohammadjavad Hamidia. 2024. "Data-Driven Crack Image-Based Seismic Failure Mode Identification for Damaged RC Columns." *Engineering Failure Analysis*: 108160.

Azhari, Samira, Amirali Mahmoodi, Amirhossein Samavi, and Mohammadjavad Hamidia. 2025. "Multi-Feature Driven Seismic Damage State Identification for Reinforced Concrete Shear Walls Using Computer Vision and Machine Learning." *Advances in Engineering Software* 199: 103796.

Azuma, Y, and O Zenriku. 1977. "Examination of AF2 Series Experimental Results." *J Struct Constr Eng* 25: 1499–1500.

Babaie Mahani, Alireza, and Javad Kazemian. 2018. "Strong Ground Motion from the November 12, 2017, M 7.3 Kermanshah Earthquake in Western Iran." *Journal of Seismology* 22(6): 1339–58.

Baduge, Shanaka Kristombu, Sadeep Thilakarathna, Jude Shalitha Perera, Mehrdad Arashpour, Pejman Sharafi, Bertrand Teodosio, Ankit Shringi, and Priyan Mendis. 2022. "Artificial Intelligence and Smart Vision for Building and Construction 4.0: Machine and Deep Learning Methods and Applications." *Automation in Construction* 141: 104440.

Barbot, Sylvain, Heng Luo, Teng Wang, Yariv Hamiel, Oksana Piatibratova, Muhammad Tahir Javed, Carla Braitenberg, and Gokhan Gurbuz. 2023. "Slip Distribution of the February 6, 2023 Mw 7.8 and Mw 7.6, Kahramanmaraş, Turkey Earthquake Sequence in the East Anatolian Fault Zone." *Seismica* 2(3).

Beckman, Gustavo H, Dimos Polyzois, and Young-Jin Cha. 2019. "Deep Learning-Based Automatic Volumetric Damage Quantification Using Depth Camera." *Automation in Construction* 99: 114–24.

Bett, Bart J, James Otis Jirsa, and Richard E Klingner. 1985. *Behavior of Strengthened and Repaired Reinforced Concrete Columns under Cyclic Deformations*. Phil M. Ferguson Structural Engineering Laboratory, University of Texas at ….

Birely, Anna C, Laura N Lowes, and Dawn E Lehman. 2011. Fema P-58-3 *FEMA P-58/BD-3.8.9 – Fragility Functions for Slender Reinforced Concrete Walls*.

Bishop, Christopher M. 1995. *Neural Networks for Pattern Recognition*. Oxford university press.

Breiman, Leo. 2001. "Random Forests." *Machine learning* 45: 5–32.

Chaudhuri, Kamalika, and Sanjoy Dasgupta. 2014. "Rates of Convergence for Nearest Neighbor Classification." *Advances in Neural Information Processing Systems* 27.

Chen, Bo, Hua Zhang, Guijin Wang, Jianwen Huo, Yonglong Li, and Linjing Li. 2023. "Automatic Concrete Infrastructure Crack Semantic Segmentation Using Deep Learning." *Automation in Construction* 152: 104950.

Chen, Qisen, Bo Yu, and Bing Li. 2024. "Quantifying Seismic Damage in RC Walls with Image Analysis." *Journal of Earthquake Engineering*: 1–24.

Committee, A C I. 2008. "Building Code Requirements for Structural Concrete (ACI 318-08) and Commentary." In American Concrete Institute.

Cordeiro, Sergio Gustavo Ferreira, and Edson Denner Leonel. 2019. "An Improved Computational Framework Based on the Dual Boundary Element Method for Three-Dimensional Mixed-Mode Crack Propagation Analyses." *Advances in Engineering Software* 135: 102689.

Cover, Thomas, and Peter Hart. 1967. "Nearest Neighbor Pattern Classification." *IEEE transactions on information theory* 13(1): 21–27.

Dung, Cao Vu. 2019. "Autonomous Concrete Crack Detection Using Deep Fully Convolutional Neural Network." *Automation in Construction* 99: 52–58.

FEMA 306. 1998. "FEMA 306. EVALUATION OF EARTHQUAKE DAMAGED CONCRETE AND MASONRY WALL BUILDINGS. Basic Procedures Manual." *Management*.

Friedman, Jerome H. 2001. "Greedy Function Approximation: A Gradient Boosting Machine." *Annals of statistics*: 1189–1232.

Fukada, Y. 1976. "Experimental Investigation of Damage in RC Columns with Various Longitudinal Rebar Arrangements." *J Struct Constr Eng* 25: 1413–14.

Géron, Aurélien. 2022. *Hands-on Machine Learning with Scikit-Learn, Keras, and TensorFlow*. " O'Reilly Media, Inc."

Grzybowski, Jacek, and Tomasz BLACHOWICZ. 2020. "Estimation of Spatial Distribution and Symmetry of Textile Materials Using Lacunarity." *Communications in Development and Assembling of Textile Products* 1(2): 180–85.

Hamidia, Mohammadjavad, Mostafa Kaboodkhani, and Hamid Bayesteh. 2024. "Vision-Oriented Machine Learning-Assisted Seismic Energy Dissipation Estimation for Damaged RC Beam-Column Connections." *Engineering Structures* 301: 117345.

Hamidia, Mohammadjavad, Sina Mansourdehghan, Amir Hossein Asjodi, and Kiarash M Dolatshahi. 2022a. "Machine Learning-Aided Scenario-Based Seismic Drift Measurement for RC Moment Frames Using Visual Features of Surface Damage." *Measurement* 205: 112195.

Hamidia, Mohammadjavad, Sina Mansourdehghan, Amir Hossein Asjodi, and Kiarash M Dolatshahi. 2022b. "Machine Learning-Based Seismic Damage Assessment of Non-Ductile RC Beam-Column Joints Using Visual Damage Indices of Surface Crack Patterns." In *Structures*, Elsevier, 2038–50.

Harirchian, Ehsan, Tom Lahmer, and Shahla Rasulzade. 2020. "Earthquake Hazard Safety Assessment of Existing Buildings Using Optimized Multi-Layer Perceptron Neural Network." *Energies* 13(8): 2060.

Hart, Peter E, David G Stork, and Richard O Duda. 2000. *Pattern Classification*. Wiley Hoboken.

Hassan, Sk S, P Pal Choudhury, B S Daya Sagar, S Chakraborty, R Guha, and A Goswami. 2015. "Quantitative Description of Genomic Evolution of Olfactory Receptors." *Asian-European Journal of Mathematics* 8(03): 1550043.

Hastie, Trevor, Robert Tibshirani, Jerome H Friedman, and Jerome H Friedman. 2009. 2 *The Elements of Statistical Learning: Data Mining, Inference, and Prediction*. Springer.

Henkhaus, Kurt W. 2010. "Axial Failure of Vulnerable Reinforced Concrete Columns Damaged by Shear Reversals."

Hu, Wenbo, Weidong Wang, Chengbo Ai, Jin Wang, Wenjuan Wang, Xuefei Meng, Jun Liu, Haowen Tao, and Shi Qiu. 2021. "Machine Vision-Based Surface Crack Analysis for Transportation Infrastructure." *Automation in Construction* 132: 103973.

Huang, Honglan, and Henry V Burton. 2019. "Classification of In-Plane Failure Modes for Reinforced Concrete Frames with Infills Using Machine Learning." *Journal of Building Engineering* 25: 100767.

Huyan, Ju, Wei Li, Susan Tighe, Junzhi Zhai, Zhengchao Xu, and Yao Chen. 2019. "Detection of Sealed and Unsealed Cracks with Complex Backgrounds Using Deep Convolutional Neural Network." *Automation in Construction* 107: 102946.

Jia, Zhe, Zeyu Jin, Mathilde Marchandon, Thomas Ulrich, Alice-Agnes Gabriel, Wenyuan Fan, Peter Shearer, et al. 2023. "The Complex Dynamics of the 2023 Kahramanmaraş, Turkey, M w 7.8-7.7 Earthquake Doublet." *Science* 381(6661): 985–90.

Lattanzi, David, Gregory R Miller, Marc O Eberhard, and Olafur S Haraldsson. 2016. "Bridge Column Maximum Drift Estimation via Computer Vision." *Journal of Computing in Civil Engineering* 30(4): 4015051.

Lim, Erwin, Shyh-Jiann Hwang, Chih-Hung Cheng, and Pin-Yi Lin. 2016. "Cyclic Tests of Reinforced Concrete Coupling Beam with Intermediate Span-Depth Ratio." *ACI Structural Journal* 113(3).

Liu, Yiqing, and Justin K W Yeoh. 2021. "Automated Crack Pattern Recognition from Images for Condition Assessment of Concrete Structures." *Automation in Construction* 128: 103765.

Liu, Zhenqing, Yiwen Cao, Yize Wang, and Wei Wang. 2019. "Computer Vision-Based Concrete Crack Detection Using U-Net Fully Convolutional Networks." *Automation in Construction* 104: 129–39.

Lynn, Abraham C, Jack P Moehle, Stephen A Mahin, and William T Holmes. 1996. "Seismic Evaluation of Existing Reinforced Concrete Building Columns." *Earthquake Spectra* 12(4): 715–39.

Mangalathu, Sujith, and Jong-Su Jeon. 2018. "Classification of Failure Mode and Prediction of Shear Strength for Reinforced Concrete Beam-Column Joints Using Machine Learning Techniques." *Engineering Structures* 160: 85–94.

de Melo, Rafael H C, and Aura Conci. 2013. "How Succolarity Could Be Used as Another Fractal Measure in Image Analysis." *Telecommunication Systems* 52(3): 1643–55.

Melo, Rafael Heitor Correia de. 2007. "Using Fractal Characteristics Such as Fractal Dimension, Lacunarity and Succolarity to Characterize Texture Patterns on Images."

Moradi, Mohammad Javad, and Mohammad Amin Hariri-Ardebili. 2019. "Developing a Library of Shear Walls Database and the Neural Network Based Predictive Meta-Model." *Applied Sciences* 9(12): 2562.

Murphy, Kevin P. 2022. *Probabilistic Machine Learning: An Introduction*. MIT press.

Mystkowski, Arkadiusz, Adam Wolniakowski, Adam Idzkowski, Maciej Ciężkowski, Michał Ostaszewski, Rafał Kociszewski, Adam Kotowski, et al. 2024. "Measurement and Diagnostic System for Detecting and Classifying Faults in the Rotary Hay Tedder Using Multilayer Perceptron Neural Networks." *Engineering Applications of Artificial Intelligence* 133: 108513.

Nanthakumar, S S, Tom Lahmer, Xiaoying Zhuang, Goangseup Zi, and Timon Rabczuk. 2016. "Detection of Material Interfaces Using a Regularized Level Set Method in Piezoelectric Structures." *Inverse Problems in Science and Engineering* 24(1): 153–76.

Nguyen, Hieu, Ngoc-Mai Nguyen, Minh-Tu Cao, Nhat-Duc Hoang, and Xuan-Linh Tran. 2021. "Prediction of Long-Term Deflections of Reinforced-Concrete Members Using a Novel Swarm Optimized Extreme Gradient Boosting Machine." *Engineering with Computers*: 1–13.

Oh, Byung Kwan, Branko Glisic, Sang Wook Park, and Hyo Seon Park. 2020. "Neural Network-Based Seismic Response Prediction Model for Building Structures Using Artificial Earthquakes." *Journal of Sound and Vibration* 468: 115109.

Okuwaki, Ryo, Yuji Yagi, Tuncay Taymaz, and Stephen P Hicks. 2023. "Multi-Scale Rupture Growth With Alternating Directions in a Complex Fault Network During the 2023 South-Eastern Türkiye and Syria

Earthquake Doublet." *Geophysical Research Letters* 50(12): e2023GL103480.

Olalusi, Oladimeji B, and Panagiotis Spyridis. 2020. "Machine Learning-Based Models for the Concrete Breakout Capacity Prediction of Single Anchors in Shear." *Advances in Engineering Software* 147: 102832.

Omor, S, T Takahashi, K Ishii, and S Watanabe. 1974. "Failure Mode of Reinforced Concrete Columns with Various Ties Configurations." *J Struct Constr Eng* 20: 1313–14.

Osamu, C, N Kondo, K Yanagishita, and R Fukuzawa. 1974. "Fracture Mechanism Identification for RC Columns with Large Height-to-width Ratios." *J Struct Constr Eng* 20: 1311–12.

Paal, Stephanie G, Jong-Su Jeon, Ioannis Brilakis, and Reginald DesRoches. 2015. "Automated Damage Index Estimation of Reinforced Concrete Columns for Post-Earthquake Evaluations."

Plotnick, Roy E, Robert H Gardner, and Robert V O'Neill. 1993. "Lacunarity Indices as Measures of Landscape Texture." *Landscape ecology* 8(3): 201–11.

Rajakarunakaran, Surya Abisek, Arun Raja Lourdu, Suresh Muthusamy, Hitesh Panchal, Ali Jawad Alrubaie, Mustafa Musa Jaber, Mohammed Hasan Ali, et al. 2022. "Prediction of Strength and Analysis in Self-Compacting Concrete Using Machine Learning Based Regression Techniques." *Advances in Engineering Software* 173: 103267.

Russell, David A, James D Hanson, and Edward Ott. 1980. "Dimension of Strange Attractors." *Physical Review Letters* 45(14): 1175.

Schapire, Robert E, and Yoav Freund. 2013. "Boosting: Foundations and Algorithms." *Kybernetes* 42(1): 164–66.

Shamsabadi, Elyas Asadi, Chang Xu, Aravinda S Rao, Tuan Nguyen, Tuan Ngo, and Daniel Dias-da-Costa. 2022. "Vision Transformer-Based Autonomous Crack Detection on Asphalt and Concrete Surfaces." *Automation in Construction* 140: 104316.

Son, Vu Ngoc. 2018. "Experimental and Analytical Investigations on Seismic Behavior of Corroded Reinforced Concrete Members."

Taud, Hind, and Jean-Franccois Mas. 2018. "Multilayer Perceptron (MLP)." *Geomatic approaches for modeling land change scenarios*: 451–55.

Tran, Cao Thanh Ngoc. 2010. "Experimental and Analytical Studies on the Seismic Behavior of Reinforced Concrete Columns with Light Transverse Reinforcement."

Vafaei, Mohammadreza, Azlan bin Adnan, and Ahmad Baharuddin Abd. Rahman. 2013. "Real-Time Seismic Damage Detection of Concrete Shear Walls Using Artificial Neural Networks." *Journal of Earthquake Engineering* 17(1): 137–54.

Wager, Stefan, and Susan Athey. 2018. "Estimation and Inference of Heterogeneous Treatment Effects Using Random Forests." *Journal of the American Statistical Association* 113(523): 1228–42.

Xia, Yuxuan, Jianchao Cai, Edmund Perfect, Wei Wei, Qi Zhang, and Qingbang Meng. 2019. "Fractal Dimension, Lacunarity and Succolarity Analyses on CT Images of Reservoir Rocks for Permeability Prediction." *Journal of Hydrology* 579: 124198.

Xiang, Chao, Wei Wang, Lu Deng, Peng Shi, and Xuan Kong. 2022. "Crack Detection Algorithm for Concrete Structures Based on Super-Resolution Reconstruction and Segmentation Network." *Automation in Construction* 140: 104346.

Yamamoto, K, and M Munemura. 1974. "Experiments on RC Short Columns with Varying Axial Force." *J Struct Constr Eng* 20: 1309–10.

Zhang, Junfei, Yuantian Sun, Guichen Li, Yuhang Wang, Junbo Sun, and Jianxin Li. 2020. "Machine-Learning-Assisted Shear Strength Prediction of Reinforced Concrete Beams with and without Stirrups." *Engineering with Computers*: 1–15.

Zhao, Peiqiang, Miao Luo, Dong Li, Yuqi Wu, Zhiqiang Mao, and Mehdi Ostadhassan. 2021. "Fractal Characterization and Petrophysical Analysis of 3D Dynamic Digital Rocks of Sandstone." *Petrophysics-The*

*SPWLA Journal of Formation Evaluation and Reservoir Description* 62(05): 500–515.

Zhou, Shuwei, Timon Rabczuk, and Xiaoying Zhuang. 2018. "Phase Field Modeling of Quasi-Static and Dynamic Crack Propagation: COMSOL Implementation and Case Studies." *Advances in Engineering Software* 122: 31–49.

Zhu, Deqi, Aiping Tang, Congli Wan, Yusheng Zeng, and Ze Wang. 2021. "Investigation on the Flexural Toughness Evaluation Method and Surface Cracks Fractal Characteristics of Polypropylene Fiber Reinforced Cement-Based Composites." *Journal of Building Engineering* 43: 103045.

Zhu, Zhenhua, Stephanie German, and Ioannis Brilakis. 2011. "Visual Retrieval of Concrete Crack Properties for Automated Post-Earthquake Structural Safety Evaluation." *Automation in Construction* 20(7): 874–83.